Original Article

Differentiation of bladder cancer stages using the vesical imaging -reporting and data system and apparent diffusion coefficient

Wei Liu[1,2#^], Ruchuan Chen[1,3#], Xiaohang Liu[1,2], Bingni Zhou[1,2], Yijun Shen[2,4], Liangping Zhou[1,2^]

[1]Department of Radiology, Fudan University Shanghai Cancer Center, Shanghai, China; [2]Department of Oncology, Fudan University Shanghai Medical College, Shanghai, China; [3]Shanghai Institute of Medical Imaging, Shanghai, China; [4]Department of Urology, Fudan University Shanghai Cancer Center, Shanghai, China

Contributions: (I) Conception and design: L Zhou, Y Shen, W Liu; (II) Administrative support: L Zhou; (III) Provision of study materials or patients: Y Shen; (IV) Collection and assembly of data: W Liu, R Chen, X Liu, B Zhou; (V) Data analysis and interpretation: W Liu, R Chen; (VI) Manuscript writing: All authors; (VII) Final approval of manuscript: All authors.

[#]These authors contributed equally to this work.

Correspondence to: Prof. Liangping Zhou, PhD, MD. Department of Radiology, Fudan University Shanghai Cancer Center, No. 270 Dongan Road, Xuhui District, Shanghai 200032, China. Email: zhoulp_2022@163.com; Prof. Yijun Shen, PhD, MD. Department of Urology, Fudan University Shanghai Cancer Center, No. 270 Dongan Road, Xuhui District, Shanghai 200032, China. Email: yijunshen79@163.com.

Background: T stage is closely related to the treatment and prognosis of patients with bladder cancer (BC). However, preoperative T staging is still challenging. Multiparametric magnetic resonance imaging (mpMRI) may be valuable. This study was performed to explore the value of the Vesical Imaging-Reporting and Data System (VI-RADS) and the volumetric apparent diffusion coefficient (ADC) histogram parameters in detecting T2 stage and below stage (≤T2 stage) from T3 stage and above stage (≥T3 stage) BCs.

Methods: The study included 62 patients (mean age, males *vs.* females: 62.1±10.9 *vs.* 61.8±11.7 years) with BC pathologically confirmed by partial or radical cystectomy. All of the tumors were scored normatively by two radiologists using the VI-RADS scoring system by two radiologists. The volumetric ADC histogram of each lesion was obtained from the ADC maps. The Cochran-Armitage test was used to examine the relevance between VI-RADS scores and T stages. The Mann-Whitney U test was used to compare the histogram parameters between ≤T2 stage and ≥T3 stage BCs. A receiver operating characteristic (ROC) curve was used to assess the predictive power of each model.

Results: The minimum ADC; mean ADC; median ADC; maximum ADC; and 10th, 25th, 75th, and 90th percentile ADC of ≤T2 stage BCs were significantly higher than those of ≥T3 stage BCs, while skewness and kurtosis had opposite results. VI-RADS achieved the highest area under the curve (AUC) of 0.834 among all parameters. The combination of VI-RADS, skewness and kurtosis yield a significantly higher AUC than VI-RADS alone (0.915 *vs.* 0.834, P=0.0478).

Conclusions: VI-RADS and volume ADC histogram analysis can effectively discriminate between ≤T2 stage and ≥T3 stage BCs, and the volumetric ADC histogram can provide further information to supplement VI-RADS.

Keywords: Bladder cancer (BC); Vesical Imaging-Reporting and Data System (VI-RADS); T stage; apparent diffusion coefficient (ADC)

^ ORCID: Wei Liu, 0000-0003-3789-8953; Liangping Zhou, 0000-0002-8638-3908.

Submitted Oct 29, 2022. Accepted for publication May 08, 2023. Published online Jun 14, 2023.
doi: 10.21037/qims-22-1184
View this article at: https://dx.doi.org/10.21037/qims-22-1184

Introduction

Bladder cancer (BC) is a common malignancy of the urinary system, and an improved understanding of molecular biology and genetics has led to the development of diagnostic and treatment methods for localized and advanced BC (1). Local invasion depth locally of BC is a prognostic biomarker and can provide a reference for clinical strategies. For localized muscle invasive bladder cancer (MIBC), radical cystectomy (RC) is a curative treatment (2). The five-year survival rate after RC is approximately 40% in patients with T2 stage BC, while it is only approximately 20% in patients with T3 stage and above (3). Neoadjuvant chemotherapy (NAC) prior to RC can promote pathological downstaging (4), and provide overall survival (OS) and disease-free survival (DFS) benefit (5), and it does not adversely affect the chances of proceeding with RC (6); therefore, NAC may become an important treatment modality for patients with localized MIBC. A study, enrolling 2,673 patients who received NAC before RC, revealed that stage cT2 patients demonstrated a more complete response on final pathology than stage cT3 and cT4 patients (7). Additionally, for some patients with MIBC, especially elderly patients, bladder-sparing strategies are worthwhile too. Trimodal therapy (TMT)—maximal transurethral removal of the tumor followed by chemoradiation—is a bladder-sparing treatment, that has a similar OS to elderly patients who undergo RC (8,9). T2 stage was significantly associated with better local control and OS for patients who underwent TMT (9,10). On this basis, identifying T2 from ≥T3 stage BC precisely before treatment shows some clinical significance.

Previously, accurate preoperative evaluation of T stage mainly relied on transurethral resection of bladder tumors (TURBT), which is invasive and unable to detect the invasion of perivesical tissue precisely. In recent years, the potential of multimodal data analysis in related clinical applications of BC has captured increasing attention, and imaging medicine is one of the essential parts (11). With the rapid development of magnetic resonance imaging (MRI), more high-resolution images and quantitative parameters, especially diffusion-weighted imaging (DWI), can be obtained, which greatly contributes to the estimation of the clinical stage, local recurrence and therapeutic response of BC. To standardize reporting and scanning of bladder MRI, the Vesical Imaging-Reporting and Data System (VI-RADS) was created by multidisciplinary experts in 2018 (12). VI-RADS on the basis of multiparametric MRI (mpMRI) showed considerable value in predicting MIBC and non-MIBC (NMIBC) in previous studies (13-15). A meta-analysis by Ye *et al.* (14), which included 17 studies with a total of 2,344 patients, concluded that VI-RADS showed sensitivities and specificities of 0.91 (95% CI: 0.87–0.94) and 0.86 (95% CI: 0.77–0.91) at a cutoff score of 3, and 0.85 (95% CI: 0.77–0.90) and 0.93 (95% CI: 0.89–0.96) at a cutoff score of 4. However, the value of mpMRI in evaluating perivesical tissue invasion which has been shown to be closely related to poor survival and prognosis (16,17) is still unclear.

Histogram analysis, describing the statistical information of the MRI parameters, can be used to estimate intratumor heterogeneity and show more reliable and accurate parameters (18). According to the above analysis, we designed this study to explore the value of VI-RADS and histogram parameters based on mpMRI in predicting the invasion of perivesical tissue.

Methods

Patient selection

This retrospective study was conducted in accordance with the Declaration of Helsinki (as revised in 2013). The study was approved by the institutional medical ethics committee of Fudan University Shanghai Cancer Center and written informed consent was waived due to the retrospective nature of the study. In this study, 195 patients who underwent bladder MRI examinations from November 2019 to July 2022 were screened retrospectively. Of these, 101 patients were excluded because they did not undergo RC or partial cystectomy (PC) after MRI examination, 17 patients were excluded due to postoperative pathological findings of nonurothelial carcinoma, and 15 patients were excluded due to poor MRI image quality (such as motion artifacts and bladder underfilling). Ultimately, 62 patients (84 independent lesions) with pathologically confirmed urothelial carcinoma were enrolled in this study. A flow diagram of the population selection process is presented in

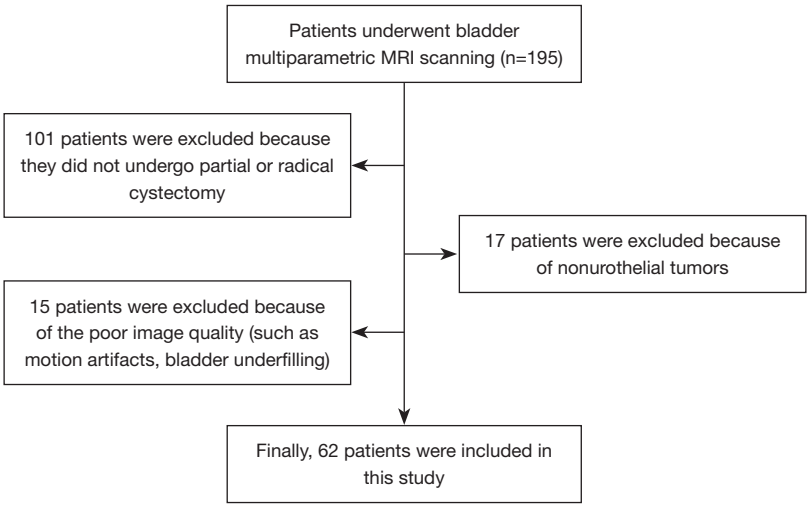

Figure 1 Flowchart showing the patient selection process. MRI, magnetic resonance imaging.

Figure 1.

Pathological T stage was determined according to the 8th American Joint Committee on Cancer Staging manual (19). When BC invaded perivesical tissues, including fat, prostatic stroma, seminal vesicles, uterus, vagina, pelvic wall, and abdominal wall, the T stage was classified as ≥T3 stage.

MpMRI examination

Patients were required to first urinate and then drink 500–1,000 mL of water over one and half hours to two hours before the MRI examination to ensure adequate filling of the bladder. The supine position was used for MRI examination. Patients were asked to fast strictly for six hours before MRI examination to avoid motion artifacts caused by intestinal motility (12).

All pelvic examinations were performed using a 3.0 T scanner (Skyra; Siemens Healthcare, Erlangen, Germany) with a 16-channel phased-array surface coil. The MRI sequences included the following parameters: (I) T1-weighted imaging (T1WI): echo time (TE), 2.46 ms; repetition time (TR), 231 ms; field of view (FOV), 30×30 cm; slice thickness (ST), 5.5 mm. (II) Sagittal T2WI: TE, 101 ms; TR, 6,760 ms; FOV, 30×30 cm; ST, 4 mm. (III) Axial T2WI: TE, 101 ms; TR, 1,500 ms; FOV, 23×23 cm; ST, 1.5 mm. (IV) Readout-segmented echo-planar (RESOLVE) DWI sequence: b values, 0 and 1,000 s/mm^2; TE, 62 ms; TR, 6,210 ms; FOV, 32 cm; ST, 4 mm. (V) Volumetric interpolated breath-hold examination (VIBE) dynamic contrast-enhanced (DCE) sequence: TE, 1.39 ms; TR, 3.56 ms; FOV, 33×20 cm; ST, 3 mm. All patients were asked to breathe quietly during the examination and to place their hands above their heads. A 0.1 mmol/kg dose of contrast agent (Gd-DTPA, Magnevist, Bayer HealthCare Pharmaceuticals Inc., Whippany, NJ, USA) was injected as an intravenous bolus at a rate of 1.5–2 mL/s, followed by a 10 mL saline flush at 2 mL/s 10 s after the beginning of the DCE sequence.

Imaging reading

All pelvic MRI data were transmitted to our workstation (AW4.6, GE Healthcare, Milwaukee, WI, USA). All MRI images for each tumor were used for the VI-RADS scoring system which strictly complies with the scoring criteria (12). The final VI-RADS scores were based on anatomical appearances in T2WI, DWI, and DCE images.

Structural category (SC) 1: uninterrupted low SI line representing the integrity of the muscularis propria (lesion size <1 cm; exophytic tumor with or without a stalk and/or a thickened inner layer).

SC 2: uninterrupted low SI line representing the integrity of muscularis propria (lesion size >1 cm; exophytic tumor with a stalk and/or a high SI thickened inner layer, when present, or sessile/broad-based tumor with high SI thickened inner layer, when present).

SC 3: lack of category 2 findings with the associated presence of an exophytic tumor without stalk, or a sessile/broad-based tumor without a high SI thickened inner layer but with no clear disruption of the low SI muscularis propria.

SC 4: interruption the of low SI line suggesting extension of the intermediate SI tumor tissue to muscularis propria.

SC 5: extension of intermediate SI tumor to extravesical tissues.

For SC 5 tumors, the clinical T stage was ≥T3 stage, or the clinical T stage was ≤T2 stage.

The scoring process was conducted independently by two radiologists with 5 and 11 years radiological diagnostic experience in the urinary system independently without knowing the pathological result. If the ultimate VI-RADS scores of the two readers were different, disagreements were resolved through negotiation between the two readers. In addition, apparent diffusion coefficient (ADC) maps for each tumor were independently analyzed by the same two urology radiologists mentioned above using FireVoxel software (NYU Center for Advanced Imaging Innovation and Research, New York, NY, USA). The regions of interest (ROIs) of each lesion were obtained by delineating the boundary of each layer of images on every tumor, avoiding necroses, and then a 3D model of every tumor was reconstructed. Finally, the volume ADC histogram of the lesion was obtained. In our study, the stalks of some lesions were included in the ROI as it was found by some researches (20,21) that there may be some association between the stalk and the depth of tumor invasion. *Figures 2*,*3* show the processes of delineating ROIs and computing the ADC histogram.

Statistical analysis

All patient data were calculated by using SPSS version 26 (Chicago, IL, USA). The intraclass correlation coefficient (ICC) with 95% confidence intervals was calculated to evaluate the consistency of interobservers. The Cochran-Armitage test was used to examine the relevance between VI-RADS scores and T stages. The Mann-Whitney U test was used to compare each volumetric ADC histogram parameter between the ≤T2 stage and ≥T3 stage BC groups. Receiver operating characteristic (ROC) curves with the area under the curve (AUC) were used to assess the ability of each parameter to predict ≤T2 or ≥T3 stage of BCs. A two-tailed P value <0.05 was considered indicative of a significant difference.

Results

Clinical and pathological data

This confirmatory study included a total of 62 patients with BC confirmed by RC or PC which included 52 men and 10 women, with a total of 84 independent lesions. The median (range) age was 65 (32 to 80) years old. Of the 84 bladder lesions, 69 (82.1%) were high-grade tumors and 15 (17.9%) were low-grade tumors. The characteristics of the 84 bladder tumors are shown in *Table 1*. According to the pathological results, the number of ≥T3 stage BC tumors was 44 (25 T3 stage tumors, 19 T4 stage tumors), and ≤T2 stage BC tumors was 40 (15 T1 stage tumors, 25 T2 stage tumors).

VI-RADS and volumetric ADC histogram analyses

As shown in *Table 2*, the ICC values of VI-RADS and ADC histogram parameters ranged from 0.836 to 0.958, which indicated that these variables showed good to excellent interobserver agreement. There was a significant correlation between VI-RADS and perivesical tissue invasion (P<0.001). There was no significant difference in entropy between the ≤T2 stage and ≥T3 stage BC groups (P=0.078). The ADC_{min}, ADC_{max}, ADC_{mean}, ADC_{median}, $ADC_{10\%}$, $ADC_{25\%}$, $ADC_{75\%}$, and $ADC_{90\%}$ values were significantly lower in the ≥T3 stage BC group than in the ≤T2 stage BC group. However, the skewness and kurtosis of the ≥T3 stage BC group were much higher, as shown in *Table 2*.

ROC analysis

All of the above independent parameters were used to draw the ROC curve, and it was shown that VI-RADS alone achieved the largest AUC (AUC =0.834), as shown in *Figure 4* and *Table 3*. Combining each of the above parameters with VI-RADS, we found that VI-RADS combined with kurtosis and skewness achieved the largest AUC, and the model was statistically significantly different from the AUC produced by VI-RADS alone (AUC =0.915, P=0.0478), as shown in *Figure 5* and *Table 4*. At the same time, the AUCs produced by the combinations of VI-RADS and anyone of ADC_{min}, ADC_{max}, ADC_{mean}, ADC_{median}, $ADC_{10\%}$, $ADC_{25\%}$, $ADC_{75\%}$, $ADC_{90\%}$, kurtosis, and skewness were not observed to be statistically significant compared with the AUC of VI-RADS alone (P=0.327, 0.180, 0.320, 0.364, 0.243, 0.0742, 0.172, 0.144, and 0.057, respectively).

Discussion

It is crucial to predict the T stage of patients with BC preoperatively, because of its value in treatment selection

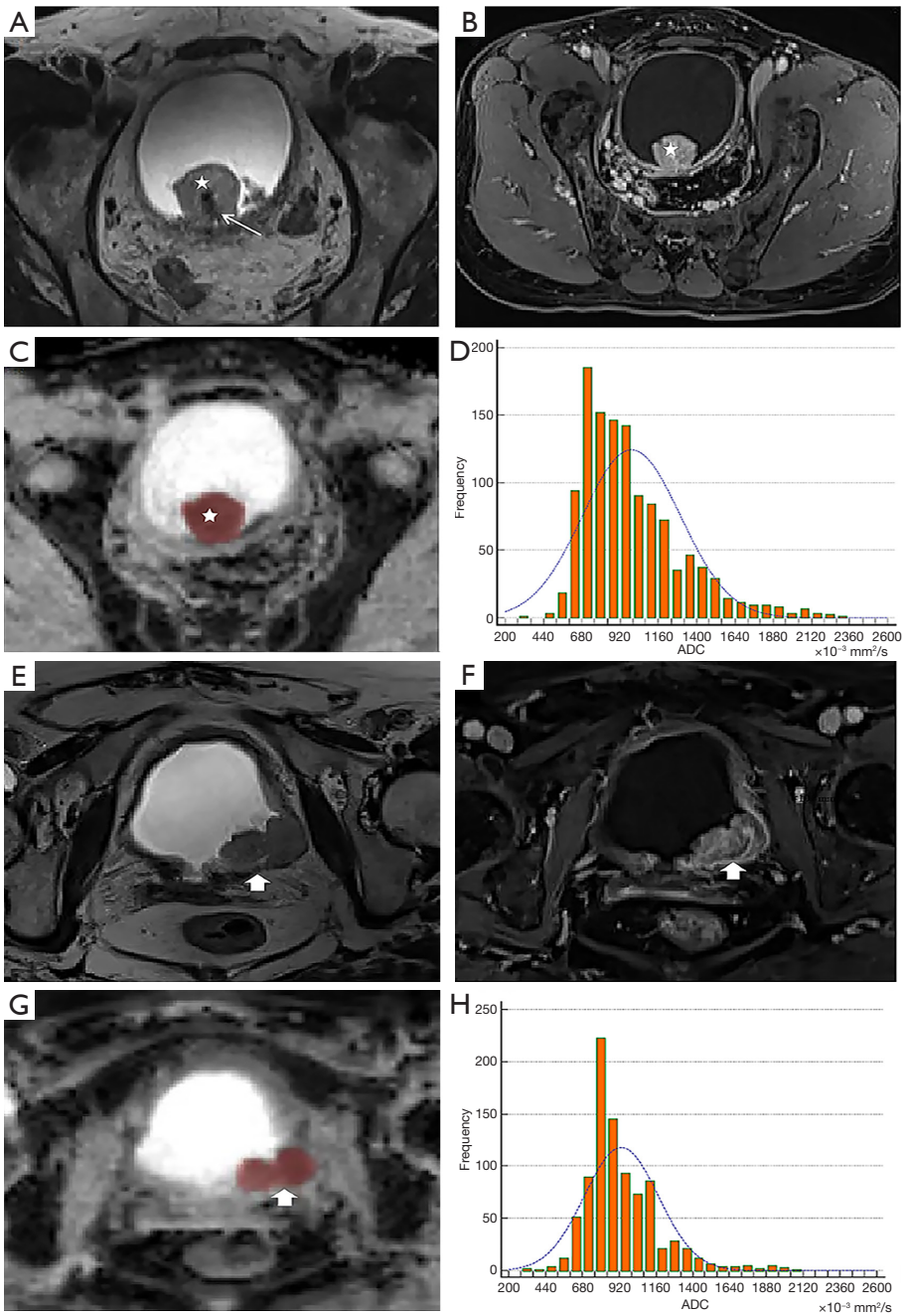

Figure 2 A 57-year-old man with T1 stage papillary urothelial carcinoma in the posterior bladder wall. The lesion (white star) had an intermediate signal on T2WI (A), was obviously enhanced in the DCE image (B) and had a low signal in the ADC map (C), and the stalk (thin white arrow) of the lesion had a low signal and was seen clearly on T2WI (A). The line signal of the bladder wall adjacent to the lesion was consecutive. The ADC histogram of the corresponding lesion is shown in (D). A 70-year-old woman with T2 stage papillary urothelial carcinoma in the left posterior bladder wall. The lesion (thick white arrow) had an intermediate signal on T2WI (E), was obviously enhanced in the DCE image (F) and had a low signal in the ADC map (G). The line signal of the bladder wall adjacent to the lesion was interrupted. The ADC histogram of the corresponding lesion was shown in (H). T2WI, T2-weighted imaging; DCE, dynamic contrast-enhanced; ADC, apparent diffusion coefficient.

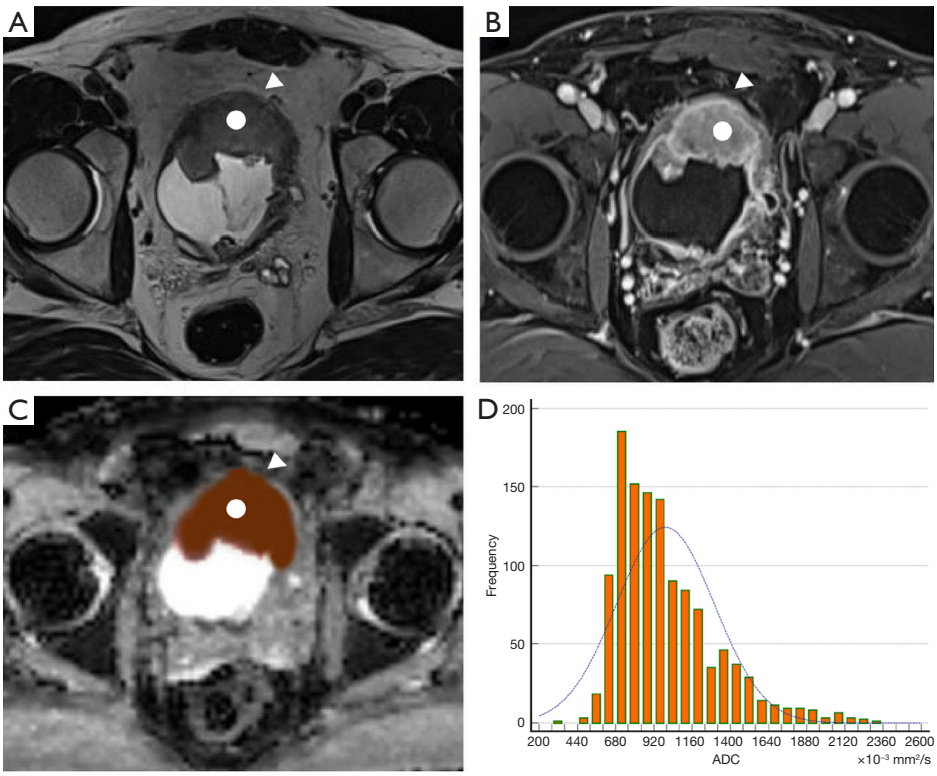

Figure 3 A 55-year-old man with T3 stage papillary urothelial carcinoma in the anterior bladder wall. The lesion (white circle) had an intermediate signal on T2WI (A), was obviously enhanced in the DCE image (B) and had a low signal in the ADC map (C). The line signal of the bladder wall adjacent to the lesion was interrupted and perivesical fat was slightly invaded (white triangle). The ADC histogram of the corresponding lesion is shown in (D). T2WI, T2-weighted imaging; DCE, dynamic contrast-enhanced; ADC, apparent diffusion coefficient.

Table 1 Characteristics of bladder tumors

Characteristics	≤T2 stage BC (n=40)	≥T3 stage BC (n=44)	Total (n=84)
VI-RADS scores			
1	1	0	1
2	2	0	2
3	9	3	12
4	24	8	32
5	4	33	37
Diameter of lesion			
>3 cm	13	26	39
≤3 cm	27	18	45
Pathological grade			
Low	9	6	15
High	31	38	69
Recurrence			
Yes	13	14	27
No	27	30	57

BC, bladder cancer; VI-RADS, vesical imaging-reporting and data system.

Table 2 Volumetric ADC histogram parameters and VI-RADS in differentiating ≤T2 stage and ≥T3 stage BCs, and the ICC values of volumetric ADC parameters and VI-RADS

Parameters	≤T2 stage BC (n=40)	≥T3 stage BC (n=44)	P values	ICC (95% CI)
$ADC_{10\%}$, $\times10^{-3}$ m^2/s	1.06±0.29	0.9±0.24	0.01	0.943 (0.921–0.969)
$ADC_{25\%}$, $\times10^{-3}$ m^2/s	1.17±0.31	1.03±0.30	0.04	0.914 (0.879–0.932)
$ADC_{75\%}$, $\times10^{-3}$ m^2/s	1.48±0.34	1.29±0.36	0.01	0.958 (0.936–0.974)
$ADC_{90\%}$, $\times10^{-3}$ m^2/s	1.76±0.32	1.48±0.36	<0.001	0.926 (0.879–0.948)
ADC_{min}, $\times10^{-3}$ m^2/s	0.92±0.27	0.71±0.25	<0.001	0.952 (0.934–0.965)
ADC_{median}, $\times10^{-3}$ m^2/s	1.35±0.29	1.18±0.32	0.01	0.905 (0.851–0.934)
ADC_{mean}, $\times10^{-3}$ m^2/s	1.39±0.29	1.17±0.29	<0.001	0.947 (0.914–0.971)
ADC_{max}, $\times10^{-3}$ m^2/s	1.94±0.39	1.64±0.33	<0.001	0.836 (0.747–0.893)
Skewness	0.87±0.66	1.11±0.62	0.01	0.865 (0.791–0.908)
Kurtosis	1.84±2.17	3.26±2.17	<0.001	0.878 (0.817–0.919)
Entropy	3.79±0.21	3.85±0.22	0.078	0.857 (0.779–0.903)
VI-RADS	4 [1, 5]	5 [3, 5]	<0.001	0.954 (0.931–0.971)

Data presented as mean ± standard deviation or median [range]. ADC, apparent diffusion coefficient; VI-RADS, vesical imaging-reporting and data system; BC, bladder cancer; ICC, intraclass correlation coefficient.

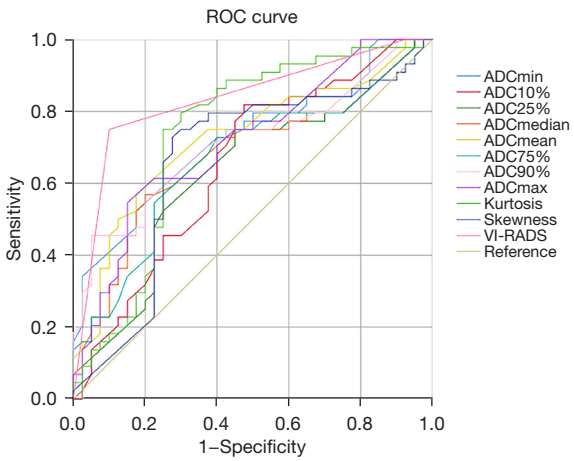

Figure 4 ROC curves of the VI-RADS score and the volumetric ADC histogram parameters. ROC, receiver operating characteristic; ADC, apparent diffusion coefficient; VI-RADS, Vesical Imaging-Reporting and Data System.

and prognosis prediction (3,22). VI-RADS, a popular tool for predicting MIBC in recent years, has achieved gratifying results (23-25), but its efficacy in differentiating ≤T2 and ≥T3 stage BCs is still controversial. In this study, we found that VI-RADS was an excellent tool for predicting ≥T3 stage BCs, and a volumetric ADC histogram can further enhance its diagnostic performance.

A previous review by Gandhi *et al.* (26) mentioned that mpMRI had a sensitivity and specificity of 0.83 and 0.87 for predicting ≤T2 and ≥T3 BC, respectively. The results of a meta-analysis by Cornelissen *et al.* (27) showed that the sensitivity and specificity of mpMRI in differentiating ≤T2 and ≥T3 BC were only 0.71 and 0.77, respectively. In our study, VI-RADS with a threshold value of 5 obtained similar sensitivity and slightly higher specificity, which may be because VI-RADS includes multiple MRI sequences and normalized preparation before examination and scanning parameters. Since this is the first time that VI-RADS has been used to predict perivesical tissue invasion of BC preoperatively, its effect needs to be further confirmed by prospective studies with a larger sample size. In addition, compared with the uneven MRI sequences in previous studies (28-30), VI-RADS can effectively provide standardized reports that are beneficial for the communication between doctors and patients.

Previous studies (31-33) have shown that there is a significant correlation between ADC values and the pathological grade of BC, and that volumetric ADC histograms can provide more lesion information than ADC values. In our study, we found that the ADC values of each percentile in the ≥T3 stage BC group were significantly lower than those in the ≤T2 stage BC group, which

Table 3 Diagnostic efficacy of VI-RADS and volumetric ADC histogram parameters in differentiating ≤T2 stage from ≥T3 stage BCs

Parameters	AUC	95% CI	Cutoff value	Sensitivity (%)	Specificity (%)	Youden index
$ADC_{10\%}$	0.653	0.541–0.754	1.05	81.82	52.50	0.3432
$ADC_{25\%}$	0.630	0.517–0.732	1.12	75.00	55.00	0.3000
$ADC_{75\%}$	0.670	0.558–0.768	1.38	72.73	60.00	0.3273
$ADC_{90\%}$	0.714	0.605–0.808	1.33	45.45	95.00	0.4045
ADC_{min}	0.724	0.616–0.816	0.67	52.27	82.50	0.3477
ADC_{median}	0.677	0.566–0.775	1.15	56.82	80.00	0.3682
ADC_{mean}	0.726	0.618–0.818	1.13	56.82	82.50	0.3932
ADC_{max}	0.717	0.608–0.810	1.64	54.55	85.00	0.3955
Skewness	0.666	0.554–0.765	0.92	72.73	72.50	0.4523
Kurtosis	0.738	0.631–0.828	1.90	75.00	75.00	0.5000
VI-RADS	0.834	0.737–0.907	5	75.00	90.00	0.6500

VI-RADS, vesical imaging-reporting and data system; ADC, apparent diffusion coefficient; AUC, area under the curve; BC, bladder cancer.

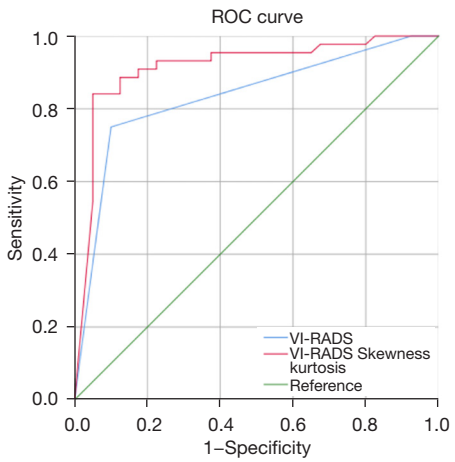

Figure 5 ROC curves of the VI-RADS score combined with the volumetric ADC histogram parameters skewness and kurtosis. ROC, receiver operating characteristic; VI-RADS, Vesical Imaging-Reporting and Data System; ADC, apparent diffusion coefficient.

reflected the more restricted diffusion of water molecules in the former group. In addition to the above quantitative ADC parameters, our study also showed that the skewness and kurtosis of the lesions in the ≥T3 stage BC group were significantly higher, which was consistent with the findings of Suo *et al.* (34). This may be because the fact that higher-stage tumors have denser cells, denser blood vessels and more disorganization (35).

Our study shows that the volume ADC histogram can provide additional diagnostic value for VI-RADS, and shows good to excellent interreader agreement, which means that the combination of the volume ADC histogram and VI-RADS has great practical value.

There are some limitations of our study. First, the nature of a retrospective study determines its inherent bias. In addition, this is a single-center study, and the sample size is limited, which may lead to some deviations in the results. Finally, we did not have data for OS and DFS, so we

Table 4 Diagnostic performance of VI-RADS score combined volumetric ADC histogram parameters

Variables	AUC	95% CI	P values
VI-RADS	0.834	0.737–0.907	–
VI-RADS_Kurtosis	0.861	0.768–0.927	0.1441
VI-RADS_Skewness	0.901	0.817–0.956	0.0569
VI-RADS_Kurtosis_Skewness	0.915	0.833–0.965	0.0478*

*, P<0.05 is considered to have a statistical difference compared with VI-RADS. VI-RADS, vesical imaging-reporting and data system; ADC, apparent diffusion coefficient; AUC, area under the curve.

could not investigate the relationship between T stage and survival. In the future, multicenter studies with large sample sizes need to be performed.

Conclusions

Both VI-RADS and volumetric ADC histograms exhibited an excellent ability to distinguish ≤T2 and ≥T3 stage BCs. ADC histogram parameters can further increase the diagnostic power of VI-RADS, especially skewness and kurtosis.

Acknowledgments

Thanks to Rong Li, Lei Yue and Zhangzhe Chen who all work at the Department of Radiology, Fudan University Shanghai Cancer Center for providing MR scanning technical support.
Funding: This study was supported by the Shanghai Anticancer Association Young Eagle Program (No. SACA-CY19C06).

Footnote

Conflicts of Interest: All authors have completed the ICMJE uniform disclosure form (available at https://qims.amegroups.com/article/view/10.21037/qims-22-1184/coif). The authors have no conflicts of interest to declare.

Ethical Statement: The authors are accountable for all aspects of the work in ensuring that questions related to the accuracy or integrity of any part of the work are appropriately investigated and resolved. This retrospective study was conducted in accordance with the Declaration of Helsinki (as revised in 2013). The study was approved by the institutional medical ethics committee of Fudan University Shanghai Cancer Center, and written informed consent was waived due to the retrospective nature of the study.

References

1. Lenis AT, Lec PM, Chamie K, Mshs MD. Bladder Cancer: A Review. JAMA 2020;324:1980-91.
2. Flaig TW, Spiess PE, Agarwal N, Bangs R, Boorjian SA, Buyyounouski MK, et al. Bladder Cancer, Version 3.2020, NCCN Clinical Practice Guidelines in Oncology. J Natl Compr Canc Netw 2020;18:329-54.
3. Reuter VE. Bladder. Risk and prognostic factors--a pathologist's perspective. Urol Clin North Am 1999;26:481-92.
4. Rose TL, Harrison MR, Deal AM, Ramalingam S, Whang YE, Brower B, Dunn M, Osterman CK, Heiling HM, Bjurlin MA, Smith AB, Nielsen ME, Tan HJ, Wallen E, Woods ME, George D, Zhang T, Drier A, Kim WY, Milowsky MI. Phase II Study of Gemcitabine and Split-Dose Cisplatin Plus Pembrolizumab as Neoadjuvant Therapy Before Radical Cystectomy in Patients With Muscle-Invasive Bladder Cancer. J Clin Oncol 2021;39:3140-8.
5. Jain RK, Sonpavde G. Neoadjuvant therapy for muscle-invasive bladder cancer. Expert Rev Anticancer Ther 2020;20:603-14.
6. Grossman HB, Natale RB, Tangen CM, Speights VO, Vogelzang NJ, Trump DL, deVere White RW, Sarosdy MF, Wood DP Jr, Raghavan D, Crawford ED. Neoadjuvant chemotherapy plus cystectomy compared with cystectomy alone for locally advanced bladder cancer. N Engl J Med 2003;349:859-66.
7. Nassiri N, Ghodoussipour S, Maas M, Nazemi A, Asanad K, Pearce S, Bhanvadia SS, Djaladat H, Schuckman A, Daneshmand S. Occult Nodal Metastases in Patients Down-Staged to Nonmuscle Invasive Disease Following Neoadjuvant Chemotherapy. Urology 2020;142:155-60.
8. Girardi DM, Ghatalia P, Singh P, Iyer G, Sridhar SS, Apolo AB. Systemic therapy in bladder preservation. Urol Oncol 2023;41:39-47.
9. Verschoor N, Heemsbergen WD, Boormans JL, Franckena M. Bladder-sparing (chemo)radiotherapy in elderly patients with muscle-invasive bladder cancer: a retrospective cohort study. Acta Oncol 2022;61:1019-25.
10. Giacalone NJ, Shipley WU, Clayman RH, Niemierko A, Drumm M, Heney NM, Michaelson MD, Lee RJ, Saylor PJ, Wszolek MF, Feldman AS, Dahl DM, Zietman AL, Efstathiou JA. Long-term Outcomes After Bladder-

preserving Tri-modality Therapy for Patients with Muscle-invasive Bladder Cancer: An Updated Analysis of the Massachusetts General Hospital Experience. Eur Urol 2017;71:952-60.
11. Wu P, Wu K, Li Z, Liu H, Yang K, Zhou R, Zhou Z, Xing N, Wu S. Multimodal investigation of bladder cancer data based on computed tomography, whole slide imaging, and transcriptomics. Quant Imaging Med Surg 2023;13:1023-35.
12. Panebianco V, Narumi Y, Altun E, Bochner BH, Efstathiou JA, Hafeez S, Huddart R, Kennish S, Lerner S, Montironi R, Muglia VF, Salomon G, Thomas S, Vargas HA, Witjes JA, Takeuchi M, Barentsz J, Catto JWF. Multiparametric Magnetic Resonance Imaging for Bladder Cancer: Development of VI-RADS (Vesical Imaging-Reporting And Data System). Eur Urol 2018;74:294-306.
13. Huang L, Kong Q, Liu Z, Wang J, Kang Z, Zhu Y. The Diagnostic Value of MR Imaging in Differentiating T Staging of Bladder Cancer: A Meta-Analysis. Radiology 2018;286:502-11.
14. Ye L, Chen Y, Xu H, Xie H, Yao J, Liu J, Song B. Biparametric magnetic resonance imaging assessment for detection of muscle-invasive bladder cancer: a systematic review and meta-analysis. Eur Radiol 2022;32:6480-92.
15. Wang H, Luo C, Zhang F, Guan J, Li S, Yao H, Chen J, Luo J, Chen L, Guo Y. Multiparametric MRI for Bladder Cancer: Validation of VI-RADS for the Detection of Detrusor Muscle Invasion. Radiology 2019;291:668-74.
16. Oz II, Altinbas NK, Serifoglu I, Oz EB, Yagci C. The Role of Computerized Tomography in the Assessment of Perivesical Invasion in Bladder Cancer. Pol J Radiol 2016;81:281-7.
17. Scosyrev E, Yao J, Messing E. Microscopic invasion of perivesical fat by urothelial carcinoma: implications for prognosis and pathology practice. Urology 2010;76:908-13; discussion 914.
18. Huang C, Zhan C, Hu Y, Yin T, Grimm R, Ai T. Histogram analysis of breast diffusion kurtosis imaging: a comparison between readout-segmented and single-shot echo-planar imaging sequence. Quant Imaging Med Surg 2023;13:735-46.
19. Magers MJ, Lopez-Beltran A, Montironi R, Williamson SR, Kaimakliotis HZ, Cheng L. Staging of bladder cancer. Histopathology 2019;74:112-34.
20. Takeuchi M, Sasaki S, Ito M, Okada S, Takahashi S, Kawai T, Suzuki K, Oshima H, Hara M, Shibamoto Y. Urinary bladder cancer: diffusion-weighted MR imaging--accuracy for diagnosing T stage and estimating histologic grade. Radiology 2009;251:112-21.
21. Yajima S, Yoshida S, Takahara T, Arita Y, Tanaka H, Waseda Y, Yokoyama M, Ishioka J, Matsuoka Y, Saito K, Kihara K, Fujii Y. Usefulness of the inchworm sign on DWI for predicting pT1 bladder cancer progression. Eur Radiol 2019;29:3881-8.
22. El-Achkar A, Souhami L, Kassouf W. Bladder Preservation Therapy: Review of Literature and Future Directions of Trimodal Therapy. Curr Urol Rep 2018;19:108.
23. Akcay A, Yagci AB, Celen S, Ozlulerden Y, Turk NS, Ufuk F. VI-RADS score and tumor contact length in MRI: A potential method for the detection of muscle invasion in bladder cancer. Clin Imaging 2021;77:25-36.
24. Feng Y, Zhong K, Chen R, Zhou W. Diagnostic accuracy of vesical imaging-reporting and data system (VI-RADS) for the detection of muscle-invasive bladder cancer: a meta-analysis. Abdom Radiol (NY) 2022;47:1396-405.
25. Kufukihara R, Kikuchi E, Shigeta K, Ogihara K, Arita Y, Akita H, Suzuki T, Abe T, Mizuno R, Jinzaki M, Oya M. Diagnostic performance of the vesical imaging-reporting and data system for detecting muscle-invasive bladder cancer in real clinical settings: Comparison with diagnostic cystoscopy. Urol Oncol 2022;40:61.e1-8.
26. Gandhi N, Krishna S, Booth CM, Breau RH, Flood TA, Morgan SC, Schieda N, Salameh JP, McGrath TA, McInnes MDF. Diagnostic accuracy of magnetic resonance imaging for tumour staging of bladder cancer: systematic review and meta-analysis. BJU Int 2018;122:744-53.
27. Cornelissen SWE, Veenboer PW, Wessels FJ, Meijer RP. Diagnostic Accuracy of Multiparametric MRI for Local Staging of Bladder Cancer: A Systematic Review and Meta-Analysis. Urology 2020;145:22-9.
28. Lista F, Andrés G, Cáceres F, Ramón de Fata F, Rodríguez-Barbero JM, Angulo JC. Evaluation of risk of muscle invasion, perivesical and/or lymph node affectation by diffusion-weighted magnetic nuclear resonance in the patient who is a candidate for radical cystectomy. Actas Urol Esp 2013;37:419-24.
29. Tekes A, Kamel I, Imam K, Szarf G, Schoenberg M, Nasir K, Thompson R, Bluemke D. Dynamic MRI of bladder cancer: evaluation of staging accuracy. AJR Am J Roentgenol 2005;184:121-7.
30. Rajesh A, Sokhi HK, Fung R, Mulcahy KA, Bankart MJ. Bladder cancer: evaluation of staging accuracy using dynamic MRI. Clin Radiol 2011;66:1140-5.
31. Li H, Liu L, Ding L, Zhang Z, Zhang M. Quantitative Assessment of Bladder Cancer Reflects Grade and Recurrence: Comparing of Three Methods of Positioning

Region of Interest for ADC Measurements at Diffusion-weighted MR Imaging. Acad Radiol 2019;26:1148-53.
32. Rosenkrantz AB, Obele C, Rusinek H, Balar AV, Huang WC, Deng FM, Ream JM. Whole-lesion diffusion metrics for assessment of bladder cancer aggressiveness. Abdom Imaging 2015;40:327-32.
33. Kobayashi S, Koga F, Kajino K, Yoshita S, Ishii C, Tanaka H, Saito K, Masuda H, Fujii Y, Yamada T, Kihara K. Apparent diffusion coefficient value reflects invasive and proliferative potential of bladder cancer. J Magn Reson Imaging 2014;39:172-8.
34. Suo ST, Chen XX, Fan Y, Wu LM, Yao QY, Cao MQ, Liu Q, Xu JR. Histogram analysis of apparent diffusion coefficient at 3.0 T in urinary bladder lesions: correlation with pathologic findings. Acad Radiol 2014;21:1027-34.
35. O'Brien T, Cranston D, Fuggle S, Bicknell R, Harris AL. Different angiogenic pathways characterize superficial and invasive bladder cancer. Cancer Res 1995;55:510-3.

Cite this article as: Liu W, Chen R, Liu X, Zhou B, Shen Y, Zhou L. Differentiation of bladder cancer stages using the vesical imaging -reporting and data system and apparent diffusion coefficient. Quant Imaging Med Surg 2023;13(8):4897-4907. doi: 10.21037/qims-22-1184

